Magnetic Properties of a Polyfluorene Derivative Containing Complexed Neodymium Ions

Alisson J. Santana,[1] Denis A. Turchetti,[1,2] Cristiano Zanlorenzi,[1] José C. R. Santos,[4] Edson Laureto,[3] Adilson J. A. De Oliveira,[4] Leni Akcelrud[1]

[1]Paulo Scarpa Polymer Laboratory (LaPPS), Chemistry Department, Federal University of Parana, POB 19081 81531-990, Curitiba, Paraná, Brazil
[2]Institute of Physics, Physics Department, São Paulo University, POB 369 13084-971, São Carlos, São Paulo, Brazil
[3]Physic Academic Department, State University of Londrina, Londrina, Paraná, 86057-970, Brazil
[4]Physics Department, Federal University of São Carlos, São Carlos, São Paulo, POB 676, 13565-905, Brazil
Correspondence to: L. Akcelrud (E-mail: akleniak@gmail.com)

Received 26 November 2018; accepted 8 January 2019; published online 22 January 2019
DOI: 10.1002/polb.24785

ABSTRACT: Poly[9,9′-dihexylfluorene-2,7-diyl)-6,6″-(2,2′:6′,2″-terpyridine)] (LaPPS75) and its complexes with neodymium were synthesized and characterized. Magnetic measurements showed that the noncomplexed polymer presented a ferromagnetic contribution due to the formation of π stacking, and that in absence of those, the ferromagnetic behavior is suppressed. The pristine polymer, the complexed one and a low-molecular-weight model compound with the same structure of the complexed site in the parent polymer were studied. The observed behavior found is presented and discussed, the most important finding was that when a conjugated chain is used as a host for the metallic ion, an amplification of four times for the magnetization is achieved, using the same metallic content for complexed polymer and model compound for comparison. © 2019 Wiley Periodicals, Inc. J. Polym. Sci., Part B: Polym. Phys. **2019**, *57*, 304–311

KEYWORDS: magnetic polymers; metal-polymer complex; neodymium; terpyridine; conjugated polymers

INTRODUCTION The electronic properties of semiconducting conjugated polymers continue to occupy a place of strong interest either in academic or technological fields of research, due to their multipurpose applications such as, LEDs,[1–4] solar cells,[5,6] and sensors[7] to cite just a few. This class of polymers may also play a role as magnetic materials,[8,9] because in nanoscale, they are of particular interest due to the growing production of high-speed computers and high-density storage devices, as hard disks.[10] Their combination with metals, affording the so-called metallopolymers, is a promising source of exploration in this line of pursuit, but advances in this field have still a long way to go. Some reports have been out about polymers bearing external transition metals[11,12] and lanthanide ions[13–17] inserted in the polymer chain.

Nevertheless, the great majority of efforts has been concerned to small molecular magnets,[18,19] doping of semiconductors,[20–23] and heterocyclic copolymers with dithiadiazole.[11,13] However, some drawbacks of those approaches still have to be overcome, mainly the poor solubility in common organic solvents, making it difficult the necessary film formation for the processing. To the best of our knowledge, the use of fluorene-[1,3,7,24–34] derived copolymers was not yet explored as magnetic materials, especially when combined with appropriated sites for complexation with metallic ions, such as terpyridine. Additionally, these materials present important solubility properties in organic solvents, with ability of film formation by usual techniques, such as casting and jet printing and advantageous mechanical properties, turning them especially attractive for technological applications.

It has been demonstrated that the magnetic exchange interactions among the metallic ions are responsible for the magnetism in polymeric complexes.[10,35,36] Particularly, there are four types of spin exchange interactions present in these materials: (a) direct exchange of pairs with fixed spin–spin distance (r), (b) superexchange through a bridge, (c) dynamic exchange in low-viscosity solution during an encounter of two radicals (or paramagnetic complexes) bearing spins and (d) exchange in pairs with flexible bridges.[37] The magnetic exchange interaction in conjugated metallopolymers occurs mainly through the polymer backbone (bridge).

Ferromagnetism has been observed previously in conjugated polymers. In a series of polythiophene derivatives such as poly(methylthiophene),[24,25] and poly(3-hexylthiophene),[9,38]

Additional Supporting Information may be found in the online version of this article.

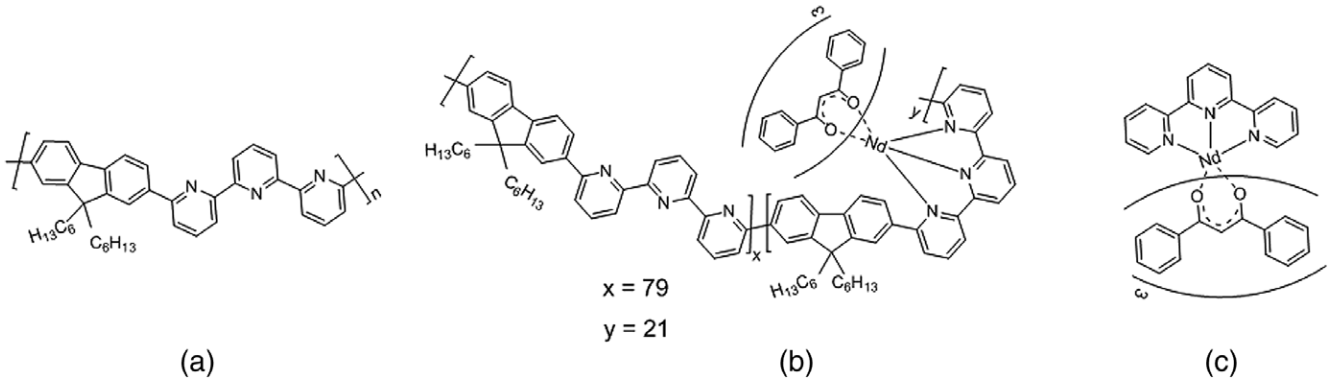

FIGURE 1 Chemical structures of the (a) pristine polymer (LaPPS75), of the (b) metallopolymer (LaPPS75Nd) and of the (c) model compound (LaPPS75M).

for example, magnetic order was demonstrated after doping, which can be made by the creation of a positive polaron in the polymer backbone with the addition of negative counter ions as perchlorate (ClO_4^-),[38] iodine,[36,39] m-chloroperbenzoic acid and[39] tetrafluoroborate (BF_4^-).[40,41] External agents have also been tried, such as pressure[38] and humidity.[9] Regioregular poly(3-hexylthiophene) (RRP3HT) and 1-(3-methoxycarbonyl) propyl-1-phenyl-[6,6]-methanefullerene (PCBM) have also shown magnetic properties in the temperature range of 5–300 K. Upon mixing those two materials, the magnetic order was suppressed and a paramagnetic signal was observed.[6]

In this article, we report on the synthesis of a organic conjugated polymer poly[9,9′-dihexylfluorene-2,7-yl)-6,6″-{2,2′:6′,2″-terpyridine)] (LaPPS75), a system that does not need any doping, neither polaron formation to show magnetic properties. The choice of neodymium as a metal for complexation was due to it is known magnetic properties in the solid state and also to the fact that this element has an electronic configuration involving the 4f levels with high quantum efficiency transitions and light emission at approximately 1060 nm. The metallopolymer was ready soluble in common organic solvents with good film-forming properties. The chemical structure of the pristine polymer (LaPPS75), of it is complexed form (LaPPS75Nd), and that of low molecular mass model compound with similar structure of the complexed sites (LaPPS75M) are shown in Figure 1(a–c), respectively. The latter was synthesized for comparison purposes.

The figure is merely illustrative, mainly regarding the case of (b), the metallopolymer: the complexed sites are randomly dispersed along the chain, and not in a blocked configuration, as it may be assumed by the representation.

EXPERIMENTAL

Materials

Potassium carbonate (Vetec, 99%), 6,6″-dibromo-2,2′:6′,2″-terpyridine (Aldrich, 90%), tetrakis(triphenylphosphine)palladium (0) (Aldrich, 99%), 9,9′-dihexylfluorene-2,7-diboronic-acid-bis (1,3-propanediol)ester (Aldrich, 97%), neodymium(lll) chloride hexahydrate (Aldrich, 99.9%). Dichloromethane (Synth, 99.5%), tetrahydrofuran (Synth, 99.8%), toluene (Aldrich, 99.3%), methanol (Aldrich, 99.6%). Deuterated chloroform, containing 1% (v/v) TMS (Sigma-Aldrich, P.A.) as standard for the NMR analyses, was used. The reagents were purchased from Sigma Chemical Co. (St. Louis, Missouri, EUA)

Measurements

^1H and ^{13}C NMR spectra were recorded on a Varian Inova-400 Instrument at 400 MHz with polymer solution containing deuterated chloroform ($CDCl_3$) and TMS as reference. The FTIR spectra were performed on KBr pellets using the BOMEM (Hartmann & Braun) MB-Series equipment scanning rate of 4000–400 cm^{-1} and 24 scans per minute. The polymer molecular weight was determined by gel permeation chromatography (GPC), using polystyrene as standards and THF HPLC as eluent. Thermogravimetric analyses (TGAs) were carried out under a nitrogen at a heating rate of 20 °C min^{-1} with Netzsch Thermisch analyzer TG 209 analyzer. Differential scanning calorimetric (DSC) measurements were performed on a Netzsch DSC 204 F1 equipment, under a nitrogen atmosphere. In the first run, the samples were heated from 20 to 200 °C and then cooled to 20 °C, with scanning rate of 10 °C min^{-1} and nitrogen flow 15 mL min^{-1}, respectively. Only the second run (cooling) was registered. UV–Vis spectra were measured on a Shimadzu UV-3101PC spectrometer in THF solution. The emission studies were measured on a Shimadzu RF–5301PC in THF solution and solid state. Magnetic characterization was performed using a quantum-design magnetometer (MPMPS3) with SQUID-VSM (vibrating sample magnetometry combine SQUID sensor) technique. Magnetization as a function of temperature (MxT) was performed using de zero-field cooling (ZFC) and field cooling (FC) protocols at 2 K min^{-1} and magnetization measurements as a function applied magnetic field (MxH) were taken up to 300 K.

Synthesis of LaPPS75

9,9′-Dihexylfluorene-2,7-diboronic-acid-bis(1,3-propanediol)ester (0.300 g, 0.597 mmol), 6,6″-dibromo-2,2′-6′-2″-terpyridine (0.233 g, 0.597 mmol) and potassium carbonate (2.21 g, 15.59 mmol) were added to a round-bottomed flask with high neck under an argon atmosphere. After three cycles of argon and vacuum, 12 mL of toluene and 4 mL of distilled water were added under stirring. Tetrakis(triphenylphosphine)-palladium(0) (0.024 g, 0.021 mmol) was dissolved in toluene

(2 mL) and added dropwise to the solution. After stirring for 72 h at 110 °C, the polymer was reprecipitated with methanol. Impurities and oligomers were eliminated by Soxhlet extraction using methanol and then acetone. The polymer was filtered and dried under vacuum for 48 h, resulting in 0.204 g of product with a yield of 68%. ^{13}C NMR ($CDCl_3$, 400 MHz): δ (ppm) 156.90, 155.98, 155.58, 152.00, 141.70, 139.10, 138.63, 137.68, 129.03, 128.22, 126.20, 121.43, 120.30, 119.29, 55.43, 40.46, 31.56, 29.79, 24.00, 22.61, 14.01. FTIR(KBr): 3056 (w), 2950 (m), 2923 (s), 2850 (s), 1566 (s), 1465 (w), 1423 (s), 1369 (w), 1305 (w), 1256 (m), 1157 (w), 1124 (m), 1080 (m), 989 (w), 792 (s), 744 (w), 634 (m), 541 (w).

Synthesis of the Metallopolymer with DBM Ligands (LaPPS75Nd)

Polymer LaPPS75 (0.080 g, 0.142 mmol), dibenzoylmethane (DBM) (0.095 g, 0.426 mmol) and triethylamine (0.240 mL) were dissolved in dried THF (20 mL) under argon. Neodymium(III) chloride hexahydrate (0.051 g, 0.142 mmol) was dissolved in methanol (3 mL) and added dropwise to the solution. After stirring for 24 h at 60 °C, the solvent was removed by slow evaporation of the reaction medium in Petri dish. The residue was washed several times with methanol to remove unreacted materials and then placed in a oven at 40 °C for drying. A yellow solid was obtained. FTIR(KBr): 3062 (w), 2927 (m), 2854 (s), 1595 (w), 1565 (w), 1517 (s), 1479 (w), 1454 (w), 1427 (m), 792 (s), 746 (w), 634 (m).

Synthesis of the Model Compound (LaPPS75M)

LaPPS75M was synthesized following the procedure described in elsewhere.[42] Briefly, 2,2′-6′,2″-terpyridine (0.080 g, 0.343 mmol), dibenzoylmethane (0.231 g, 1.029 mmol) and 0.2 mL of triethylamine were dissolved in dry THF (20 mL) under argon. Neodymium(III) chloride hexahydrate (0.123 g, 0.343 mmol) was dissolved in methanol (3 mL) and added dropwise to the solution. After stirring for 24 h at 60 °C, the solvent was removed by slow evaporation of the reaction medium in Petri dish. The residue was washed several times with methanol and hexane to remove unreacted materials and then placed in a vacuum oven at 40 °C for drying. A white solid was obtained. FTIR(KBr): 3058 (w), 3023 (w), 1598 (s), 1554 (s), 1514 (s), 1477 (m), 1458 (s), 1413 (s), 1307 (m), 1216 (m), 1066 (m), 1024 (w), 765 (w), 723 (m), 690 (m), 607 (w), 515 (w).

Preparation of Films of the LaPPS75Nd

The LaPPS75Nd powder was dissolved in toluene to give a 30 mg mL^{-1} solution. The solution was heated at 40 °C for 30 min. The films were obtained by casting after the total evaporation of the solvent at 90 °C.

Preparation of Films of the LaPPS75M

The solid solution of LaPPS75M in poly(methylmethacrylate) (PMMA) was prepared by mixing a 1% toluene solution of PMMA with the required amount of the complex to give a 30 mg mL^{-1} final solution. The mixture was maintained at 40 °C for 30 min with stirring. The resulting clear solution

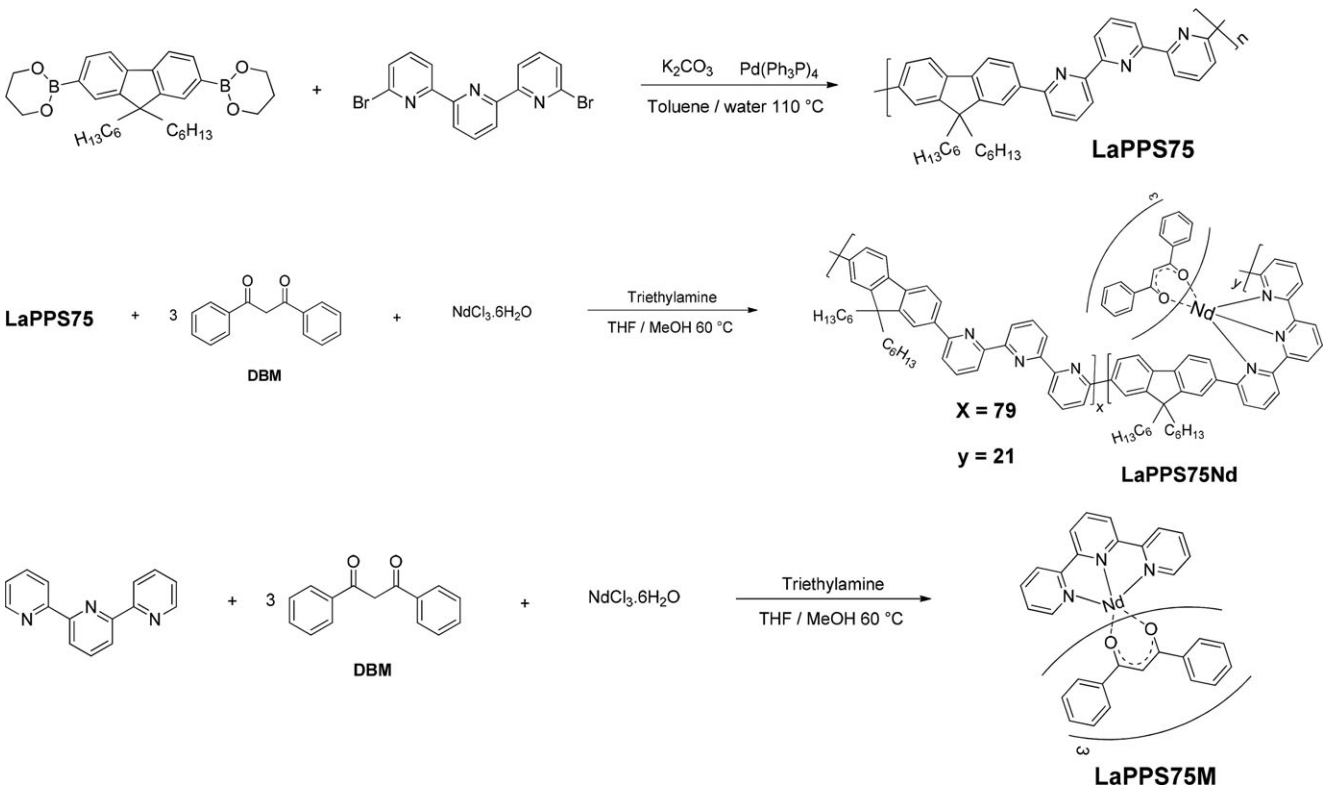

SCHEME 1 Chemical routes for the synthesis of the materials.

was cast on a Petri dish and evaporated at 40 °C in a vacuum oven until, dry giving transparent self supporting films.

The chemical pathways for the synthesis above described are illustrated in Scheme 1.

Theoretical Calculations

To optimized ground state geometry of LaPPS75, both cis–cis and trans–trans forms were determined with the density functional theory (DFT), using B3LYP functional and 6–31 g basis set as implemented in the Gaussian 09 package.[43] Based on the optimized conformer geometries, the free energies of the structures were determined.

RESULTS AND DISCUSSION

Structural Characterization

LaPPS75 was prepared through the cross-coupling Suzuki polycondensation, as shown in Scheme 1. A weight average molecular weight Mw = 21,350 g mol^{-1} was obtained, with polydispersity 1.68. Both forms of the polymer, complexed and noncomplexed presented good solubility in organic solvents such as chloroform, tetrahydrofuran, dichloromethane and so on.

The chemical structure was confirmed by ^{1}H and ^{13}C NMR and FTIR, as described in the Experimental Section and shown in the Supporting Information. Thermal stability measured by thermal gravimetric analysis (TGA) showed that the degradation temperatures ($Td_{5\%}$) (Fig. S1 in the Supporting Information) were 223 °C (LaPPS75), 228 °C (LaPPS75M) and 233 °C (LaPPS75Nd), respectively. The mass losses after the first one were different, due to the diverse bond energies of the chemical groups of each material. It is worth mentioning that the increase in the glass transition of 132 °C in the LaPPS75 to the 192 °C in the LaPPS75Nd (Fig. S2 in the Supporting Information) indicating a chain stiffening by the ion incorporated to the backbone.[42] Also, the metallopolymer shows two glass transitions, one of which matches that of the pristine, noncomplexed material and is therefore qualitatively consistent with the relatively low-complex content. The complex content, determined by TGA (oxide residue) gave a value of 21%, in a molar basis, meaning that for each 100 repeating unit is, 21 are complexed.[42,44]

Regarding the FTIR for LaPPS75 and its complexes, the main absorption bands appear at 1425 cm^{-1} and 1566 cm^{-1}, assigned to the ν(C═C) and ν(C═N) stretching vibrations,[45,46] respectively (Fig. S3 in the Supporting Information). In the spectra of the complexed materials, three characteristic bands were prominent, in the range of 1415 cm^{-1} to 1600 cm^{-1}, assigned to ν(C═C), ν(C═N) and ν(C═O) stretching vibrations, the latter one was assigned to the DBM ligand. ν(C═C), from the aromatic rings practically do not change for the polymers, complexed and pristine (1427 cm^{-1} and 1425 cm^{-1}), encompassing the vibrations of fluorene and terpyridine. For the model compound, the absorption is due only to the pyridine rings and appears at 1413 cm^{-1}. This displacement could be accounted to the coordination with the lanthanide ion, which influences the reduced mass and the force constant of the bonds. A new band at 1518 cm^{-1} may also be observed in the metallopolymer, correlated to the coordinated terpyridine sites. The displacement of the C═N bands with complexation (from 1514 cm^{-1} to 1518 cm^{-1}) was also observed in other similar systems.[42]

Photophysical Properties

The normalized absorption spectra of LaPPS75M and of LaPPS75Nd in THF solution are showed in Figure 2(a). For both, the characteristic bands of the ligand and the Nd ion were observed. Due to the low content of the complexed sites, the backbone part of the spectra falls out of scale. The complete absorption graphs are shown in the Supporting Information Figure S4. However, our main concern is to analyze the neodymium absorption in the range of 500–850 nm. Those are originated from the ground state $^{4}I_{9/2}$ to the various excited states.[47–49] All transitions relative to the absorption of

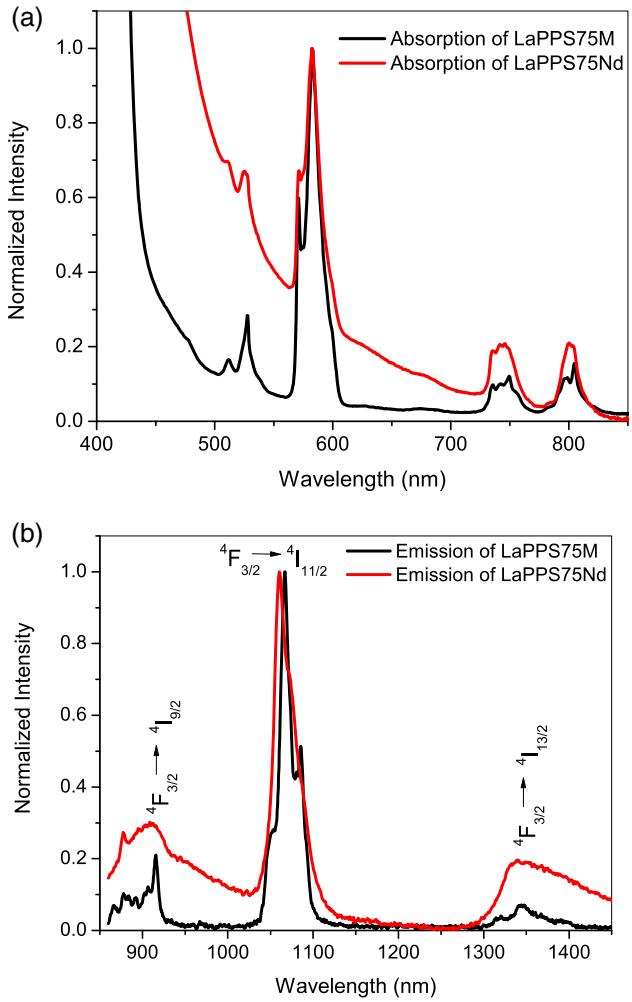

FIGURE 2 (a) Absorption spectra of LaPPS75Nd (red line, THF solution 3 × 10^{-3} mol L^{-1}) and of the model compound (LaPPS75M, black line, 3 × 10^{-3} mol L^{-1}) and (b) emission spectra of LaPPS75M dispersed in PMMA matrix and LaPPS75Nd in film form, from a drop-casting of toluene solution (30 mg mL^{-1}). The excitation source was a laser emitting at 514 nm, with power of 12 mW. [Color figure can be viewed at wileyonlinelibrary.com]

the Nd ion with the corresponding wavelengths are presented in Table S1 of the Supporting Information.

The absorption spectrum of the LaPPS75Nd does not differ significantly to that of the model compound, the location of the bands is about the same. Comparing the observed transition intensities of Figure 2(a) with those relative to the reported Nd:YAG,[50] it is noticeable that they differ considerably. For Nd:YAG, the strongest absorption is due to the $^4I_{9/2} \rightarrow {}^4F_{5/2} + {}^2H_{9/2}$ transition (775–800 nm), whereas in this case, the $^4I_{9/2} \rightarrow {}^4G_{5/2} + {}^2G_{7/2}$ (565–610 nm) transitions are the most prominent. Differences alike were also verified when other hosts are used for the Nd ion[51] and were accounted to the coordination structure of the metal with respect to the host.

Figure 2(b) shows the emission spectrum of the metallopolymer and the model compound. The dispersion in PMMA was done because LaPPS75M is a low-molecular-weight compound and as such was not able to form a film by itself. For model compound, the three emission bands characteristic of the Nd ion were observed in the NIR, centered at 915, 1067 and 1348 nm which were assigned to the $^4F_{3/2} \rightarrow {}^4I_{9/2}$, $^4F_{3/2} \rightarrow {}^4I_{11/2}$ and $^4F_{3/2} \rightarrow {}^4I_{13/2}$ transitions, respectively. The strongest of all is the $^4F_{3/2} \rightarrow {}^4I_{11/2}$ transition. The emission of the LaPPS75Nd also presented three characteristic bands of the Nd ion, with a blue shift and a broadening of the excited states in relation to LaPPS75M [Fig. 2(b)]. The bands are located at 908, 1060 and 1339 nm which were accounted for the $^4F_{3/2} \rightarrow {}^4I_{9/2}$, $^4F_{3/2} \rightarrow {}^4I_{11/2}$ and $^4F_{3/2} \rightarrow {}^4I_{13/2}$ transitions, respectively. The observed spectral changes may indicate the occurrence of alterations in the local coordination structure of the Nd^{3+}, due to interactions with the conjugation band of the polymer chain, resulting in the diminishing of the polarizability, as commented in the literature.[42,52]

Magnetic Properties

A diamagnetic character was expected for the pristine polymer (LaPPS75), as usual for semiconducting materials,[53] which was indeed seen in the magnetization vs magnetic field curve (MxH), as shown in Figure 3(a). Nevertheless, even considering that the magnetic response in 300 K is dominated by diamagnetism, at 5 K, a change in the magnetic response was observed.

Figure 3(a) presents MxH curves performed at 5 and 300 K for LaPPS75. At high temperature, a diamagnetic contribution was observed in the whole range of the applied magnetic field. This behavior was also present at low temperature superimposed with ferromagnetic and paramagnetic. The ferromagnetic contribution is associated with hysteresis observed at 5 K [inset Fig. 3(a)], with coercive field (Hc) = 180 Oe. On the other hand, the paramagnetic contribution is associated with a high saturation field, around 20 kOe. In Figure 3(b), the magnetization as a function of temperature performed using ZFC and FC protocol with H = 100 Oe is shown. The thermomagnetic irreversibility present in this measurement is associated with a small interaction between magnetic moments in the sample. In fact, the sample presents coupling and uncoupling magnetic moments, and as consequence, exhibits

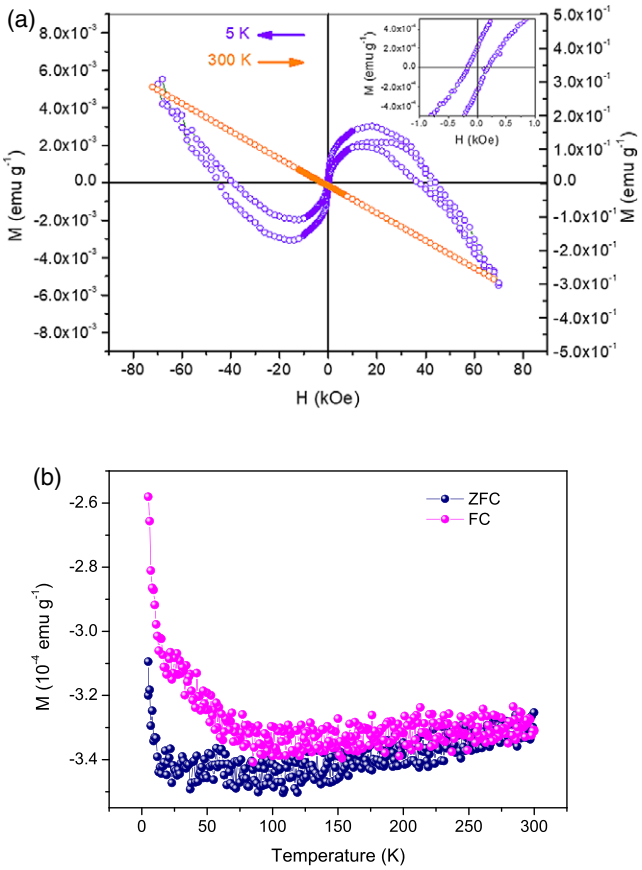

FIGURE 3 (a) Magnetization as a function of the applied field at 5 K (violet) and at 300 K (orange) for LaPPS75 in powder form. The inset shows an expanded view of the region at low field. (b) Magnetization as a function of the temperature measurements, using the procedure zero-field-cooled (ZFC) (navy blue) and field-cooled (FC) (magenta) with an applied field of 100 Oe. [Color figure can be viewed at wileyonlinelibrary.com]

simultaneous paramagnetic and ferromagnetic moments, as well as a strong diamagnetic contribution, associates to a part of the sample without magnetic moments.

Table 1 summarizes the comparative results of the magnetic properties of LaPPS75 with some works of the literature. It is worth mentioning that the material presented similar coercive field values to the reported ones, without the need of doping.

In order to compare the magnetic behavior of the neodymium linked to low-molecular-weight ligands and its metallopolymer, the magnetization curves of both materials in function of the applied field were measured. Figure 4 shows the paramagnetic behavior at 5 K for both LaPPS75M and LaPPS75Nd. When comparing the two curves, it is clearly seen that LaPPS75Nd has higher magnetization induced by the H field than LaPPS75M. This explains the greater remanence of the LaPPS75Nd, as result of the greater contribution of paramagnetic spins.

The maximum values for magnetization (M) were 4.26 and 5.88 emu g^{-1} for LaPPS75M and for LaPPS75Nd, respectively.

TABLE 1 Magnetic Properties of LaPPS75 and Literature Results at Temperature of 5 K

Conjugated polymer	Coercive field (Oe)	References
LaPPS75	180	This study
Poly(3-hexylthiophene)	80	De Paula et al.[38]
Poly(3-methylthiophene)	170	Pereira et al.[54]
Poly(3-methylthiophene)	130	Nascimento et al.[55]
Poly(N-perfluorophenylpyrrole)	373	Čík et al.[56]

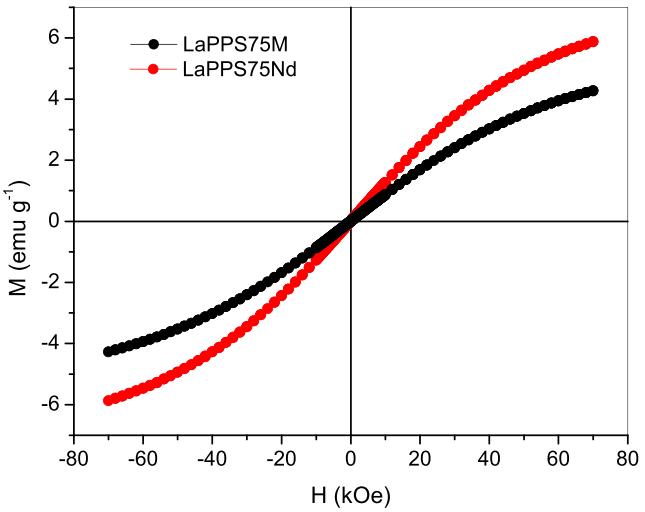

FIGURE 4 Magnetization in function of the applied field at 5 K for LaPPS75Nd (red) and LaPPS75M (black) in powder form. [Color figure can be viewed at wileyonlinelibrary.com]

The observed increase in M suggests that the complexation of rare earths, with β-diketones as ligands, can effectively alter the magnetic moment of this class of materials. The observed results for the ferromagnetic contribution could be accounted to the possible conformations of the terpyridine moiety.[57,58] It is known that the magnetic properties are strongly dependent of the ordering in the sample,[36,40] and for terpyridine moiety, three different conformations are possible: trans–trans, cis–trans and cis–cis,[45,57] each one with different bond angles between the rings. The trans–trans conformation is the most stable, with a quasi planar geometry[57,58] and the cis–cis conformation the less stable, as shown by the theoretical calculations results, as shown in Figure 5. Using the ground-state geometries of monomers, the calculated free energy difference, between the conformers trans–trans and cis–cis presented a value of 63 kJ mol^{-1}. This situation is the most favorable to π–π stacking, and according to published data,[59] a good interaction between the applied magnetic field and the polymer backbone is obtained when the chains are aggregated. Therefore, the origin of the ferromagnetic behavior in low temperatures of the pure LaPPS75 could be accounted to π–π stacking formation,[60] where the trans–trans configuration is closest to the coplanar.

The decrease in the magnetic response of the metallopolymer as compared to the pristine material was attributed to the loss of the overlap among the π clouds brought about by the bulky complexed site. This argument was also used to account for the magnetic results reported in a recent publication[60] for similar systems, indicating that π stacking is a favorable factor for the enhancement of the magnetic properties. Morphological effects on the packing of conjugated polymer chains have been addressed in a number of publications.[44,45,61,62]

In the present case, the inter-chain stacking was evidenced by the classic behavior found in the photophysical behavior of conjugated polymers, which is a progressive red shift with concentration, going from diluted conditions to the solid, as it can be clearly shown in Figure S5 of Supporting Information. The red shift is so pronounced that the first peak at 370 nm completely disappears in concentrated conditions, whereas the one in the region centered at 390 nm attributed to the stacked chains is prominent in the whole spectra. This behavior is well documented in the literature.[30–33] Additionally, the slow solvent evaporation during the sample preparation, together with the fact that the most favorable configuration of the terpyridine moiety in solution is the trans–trans, the closest to coplanar, are favorable conditions for the interchain

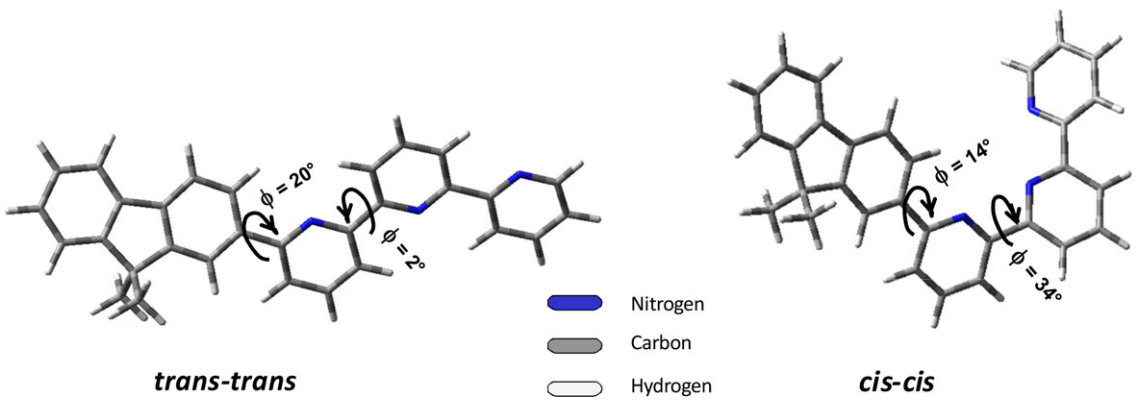

FIGURE 5 The two conformations of the terpyridine rings in the polymer: (a) trans–trans, (b) cis–cis and the corresponding dihedral angles. [Color figure can be viewed at wileyonlinelibrary.com]

stacking. Its interruption led to a dominant paramagnetic behavior as observed in Figure 4 especially at low temperatures.

Another interesting point was that converting the Nd content, mainly responsible to magnetic field, expressed in emu g^{-1} to emu mol^{-1}, one gets 4.116×10^6 emu mol^{-1} for complexed polymer and 0.887×10^6 emu mol^{-1} for the low-molecular-weight counter part. That is, for the same amount of Nd ions, the magnetic response observed is four times greater when the lanthanide is bound to a conjugated chain. The observed phenomenon represents a proof that the use of a conjugated chain amplifies four times the material´s magnetization response. It also indicates that the mechanisms operating in conjugated polymers differ of those relative to low-molecular-weight compounds, due to the interaction of the mobile electrons of the rare earth metal and the conducting band of the polymer.[19,20]

CONCLUSIONS

Magnetic measurements showed that pristine LaPPS75 exhibit is weak ferromagnetic behavior, mixed with paramagnetic and diamagnetic. When the Nd ions or atoms are added and bound to its chain, causing the loss of overlapping π clouds, the ferromagnetic component is suppressed and the samples begin to exhibit paramagnetic behavior, which is best observed at low temperatures. The interaction mechanism between the mobile electrons of the rare earth metal and those of the conjugated polymer affords and enhancement of four times of the magnetic response as compared to low-molecular-weight compounds.

ASSOCIATED CONTENT

Additional results for ^1H and ^{13}C NMR spectra, infrared spectra, thermogravimetric data, DSC curves and absorption and emission spectra of the materials.

ACKNOWLEDGMENTS

This study was financed in part by the Coordenação de Aperfeiçoamento de Pessoal de Nível Superior – Brasil (CAPES) – Finance Code 001. The authors wish to acknowledge to UFPR (Federal University of Parana), CNPq (National Council for Scientific and Technological Development), National Institute for Organic Electronics (INEO), GSM— Group of Superconductivity and Magnetism (UFSCAR) and Laboratory of Optics and Optoelectronics (UEL).

REFERENCES AND NOTES

1 L. Akcelrud, *Prog. Polym. Sci.* **2003**, *28*, 875.

2 J. C. Germino, J. N. Freitas, R. A. Domingues, F. J. Quites, M. M. Faleiros, T. Dib, Z. Atvars, *Synth. Met.* **2018**, *241*, 7.

3 D. De Azevedo, J. N. Freitas, R. A. Domingues, M. M. Faleiros, T. Dib, Z. Atvars, *Synth. Met.* **2017**, *233*, 28.

4 C. Chakraborty, A. Layek, P. P. Ray, S. Malik, *Eur. Polym. J.* **2014**, *52*, 181.

5 S.-I. Na, S.-H. Oh, S.-S. Kim, D.-Y. Kim, *Org. Electron.* **2009**, *10*, 496.

6 C. Zanlorenzi, L. Akcelrud, *J. Polym. Sci. Part B Polym. Phys.* **2017**, *55*, 919.

7 W. Gao, M. Yan, S. Ge, X. Liu, J. Yu, *Spectrochim. Acta - Part A Mol. Biomol. Spectrosc.* **2012**, *95*, 218.

8 P. Gangopadhyay, G. Koeckelberghs, A. Lopez-santiago, R. A. Norwood, *Linear Nonlinear Opt. Org. Mater. IX* **2009**, *7413*, 74130F.

9 F. R. Paula, E. C. Pereira, A. J. A. Oliveira, *J. Supercond. Nov. Magn.* **2010**, *23*, 127.

10 G. V. S. Jayapala Rao, T. N. V. K. V. Prasad, S. Shameer, M. Purnachandra Rao, *J. Magn. Magn. Mater.* **2018**, *451*, 159.

11 L. Jiang, W. Sun, J. Weng, Z. Shen, *Polymer (Guildf).* **2001**, *43*, 1563.

12 S. Reich, P. Goldberg, *J. Polym. Sci. Part B Polym. Phys.* **1983**, *21*, 869.

13 J. Tang, L. Jiang, W. Sun, Z. Shen, *React. Funct. Polym.* **2004**, *61*, 405.

14 D. Z. Liu, W. L. Sun, R. Ren, Y. H. Wang, Z. Shen, *Chin. J. Polym. Sci.* **2016**, *34*, 910.

15 B. He, W. Sun, M. Wang, Z. Shen, *Mater. Chem. Phys.* **2004**, *87*, 222.

16 J. Yang, W. Sun, Z. Zhou, Z. Shen, *J. Appl. Polym. Sci.* **2006**, *101*, 443.

17 I. Scarlatescu, M. Spunei, A. Chis, S. Negru, M. Bunoiu, N. Avram, *J. Polym. Sci. Part B: Polym. Phys.* **2006**, *44*, 3121.

18 P. Zhang, Y. N. Guo, J. Tang, *Coord. Chem. Rev.* **2013**, *257*, 1728.

19 L. Ungur, S.-Y. Lin, J. Tang, L. F. Chibotaru, *Chem. Soc. Rev.* **2014**, *43*, 6894.

20 M. C. Dimri, H. Khanduri, H. Kooskora, J. Subbi, I. Heinmaa, A. Mere, J. Krustok, R. Stern, *Phys. Status Solidi Appl. Mater. Sci.* **2012**, *209*, 353.

21 N. Pradhan, S. Das Adhikari, A. Nag, D. Sarma, *Angew. Chem. - Int. Ed.* **2017**, *56*, 7038.

22 T. A. Abdel-Baset, Y.-W. Fang, B. Anis, C.-G. Duan, M. Abdel-Hafiez, *Nanoscale Res. Lett.* **2016**, *11*, 115.

23 S. Venkatachalam, K. V. C. Rao, P. T. Manoharan, *J. Polym. Sci. Part B: Polym. Phys.* **1994**, *32*, 37.

24 A. Charas, H. Alves, J. M. G. Martinho, L. Alcácer, O. Fenwick, F. Cacialli, J. Morgado, *Synth. Met.* **2008**, *158*, 643.

25 S. P. Mucur, C. Kök, H. Bilgili, B. Canımkurbey, S. Koyuncu, *Polymer (United Kingdom)* **2018**, *151*, 101.

26 Y. Zhang, Z. Huang, W. Zeng, Y. Cao, *Polymer (Guildf).* **2008**, *49*, 1211.

27 B. Liu, W. L. Yu, Y. H. Lai, W. Huang, *Opt. Mater. (Amst).* **2003**, *21*, 125.

28 Y. Xu, H. Wang, X. Liu, Y. Wu, Z. Gao, S. Wang, Y. Miao, M. Chen, B. Xu, *J. Lumin.* **2013**, *134*, 858.

29 G. Nie, Q. Guo, Y. Zhang, S. Zhang, *Eur. Polym. J.* **2009**, *45*, 2600.

30 P. L. Santos, L. A. Cury, F. B. Dias, A. P. Monkman, *J. Lumin.* **2016**, *172*, 118.

31 T. Q. Nguyen, V. Doan, B. J. Schwartz, *J. Chem. Phys.* **1999**, *110*, 4068.

32 M. Bajpai, R. Srivastava, R. Dhar, R. S. Tiwari, *Mater. Sci. Eng. B Solid-State Mater. Adv. Technol.* **2016**, *212*, 62.

33 J. R. Tozoni, F. E. G. Guimarães, T. D. Z. Atvars, B. Nowacki, L. Akcelrud, T. J. Bonagamba, *Eur. Polym. J.* **2009**, *45*, 2467.

34 L. Akcelrud, In *In Physical Properties of Polymers Handbook*, 2nd ed.; J. E. Mark, Ed.; Springer: Cincinnati, **2007**, p. 757.

35 A. Rajca, J. Wongsriratanakul, S. Rajca, *Science* **2001**, *294*, 1503.

36 N. A. Zaidi, S. R. Giblin, I. Terry, A. P. Monkman, *Polymer (Guildf)* **2004**, *45*, 5683.

37 G. Likhtenshtein, *Electron Spin Interactions in Chemistry and Biology*; Springer: Switzerland, **2016**.

38 F. R. De Paula, D. Schiavo, E. C. Pereira, A. J. A. De Oliveira, *J. Magn. Magn. Mater.* **2014**, *370*, 110.

39 A. Ito, K. I. Ota, K. Tanaka, T. Yamabe, K. Yoshizawa, *Macromolecules* **1995**, *28*, 5618.

40 O. R. Nascimento, A. J. A. De Oliveira, E. C. Pereira, A. A. Correa, L. Walmsley, *J. Phys. Condens. Matter* **2008**, 20, 035214.

41 H. Kiess, G. Harbeke, W. Berlinger, K. W. Blazey, K. A. Moller, *Synth. Met.* **1988**, *22*, 317.

42 D. A. Turchetti, M. M. Nolasco, D. Szczerbowski, L. D. Carlos, L. C. Akcelrud, *Phys. Chem. Chem. Phys.* **2015**, *17*, 26238.

43 M.J. Frisch, G.W. Trucks, H.B. Schlegel, G.E. Scuseria, M. A. Robb, J.R. Cheeseman, G. Scalmani, V. Barone, B. Mennucci, G. A. Petersson, H. Nakatsuji, M. Caricato, X. Li, H.P. Hratchian, A. F. Izmaylov, J. Bloino, G. Zheng, J.L. Sonnenberg, M. Hada, M. Ehara, K. Toyota, R. Fukuda, J. Hasegawa, M. Ishida, T. Nakajima, Y. Honda, O. Kitao, H. Nakai, T. Vreven, J.A. Montgomery, J.E. Peralta, F. Ogliaro, M. Bearpark, J.J. Heyd, E. Brothers, K.N. Kudin, V.N. Staroverov, T. Keith, R. Kobayashi, J. Normand, K. Raghavachari, A. Rendell, J.C. Burant, S.S. Iyengar, J. Tomasi, M. Cossi, N. Rega, J.M. Millam, M. Klene, J.E. Knox, J.B. Cross, V. Bakken, C. Adamo, J. Jaramillo, R. Gomperts, R.E. Stratmann, O. Yazyev, A.J. Austin, R. Cammi, C. Pomelli, J.W. Ochterski, R.L. Martin, K. Morokuma, V.G. Zakrzewski, G.A. Voth, P. Salvador, J.J. Dannenberg, S. Dapprich, A.D. Daniels, O. Farkas, J.B. Foresman, J.V. Ortiz, J. Cioslowski, D.J. Fox, Gaussian 09, (Revision A.01), Gaussian Inc., Wallingford, CT, **2010**.

44 D. A. Turchetti, R. A. Domingues, C. Zanlorenzi, B. Nowacki, T. D. Z. Atvars, L. C. Akcelrud, *J. Phys. Chem. C* **2014**, *118*, 30079.

45 E. C. G. Campos, C. Zanlorenzi, B. F. Nowacki, G. M. Miranda, D. A. Turchetti, L. C. Akcelrud, *Adv. Condens. Matter Phys.* **2018**, 2018, 9.

46 Z. Demircioğlu, A. E. Yeşil, M. Altun, T. Bal-Demirci, N. Özdemir, *J. Mol. Struct.* **2018**, *1162*, 96.

47 C. Madhukar Reddy, N. Vijaya, D. P. Raju, *Spectrochim. Acta - Part A Mol. Biomol. Spectrosc.* **2013**, *115*, 297.

48 S. Shi, Q. Shi, C. Cui, L. Wang, Y. Tian, P. Huang, *RSC Adv.* **2016**, *6*, 91127.

49 B. Chen, J. Xu, N. Dong, H. Liang, Q. Zhang, M. Yin, *Spectrochim. Acta - Part A Mol. Biomol. Spectrosc.* **2004**, *60*, 3113.

50 U. Demirbas, A. Kurt, A. Sennaroglu, E. Yilgör, I. Yilgör, *Polymer (Guildf)* **2006**, *47*, 982.

51 S. H. Lin, R. J. Feuerstein, A. R. Mickelson, *J. Appl. Phys.* **1996**, *79*, 2868.

52 O. L. Malta, H. J. Batista, L. D. Carlos, *Chem. Phys.* **2002**, *282*, 21.

53 L. Garrido, *J. Polym. Sci. Part B: Polym. Phys.* **2010**, *48*, 1009.

54 E. C. Pereira, A. A. Correa, L. O. S. Bulhões, P. C. Aleixo, J. A. Nóbrega, A. J. A. De Oliveira, W. A. Ortiz, L. Walmsley, *J. Magn. Magn. Mater.* **2001**, *226-230*, 2023.

55 O. R. Nascimento, A. J. A. de Oliveira, A. A. Correa, L. O. S. Bulhões, E. C. Pereira, V. M. Souza, L. Walmsley, *Phys. Rev. B - Condens. Matter Mater. Phys.* **2003**, *67*, 1.

56 G. Čík, F. Šeršeň, L. Dlháň, P. Zálupský, P. Rapta, K. Hrnčariková, T. Plecenik, *J. Magn. Magn. Mater.* **2015**, *391*, 116.

57 C. Bazzicalupi, A. Bencini, A. Bianchi, A. Danesi, E. Faggi, C. Giorgi, S. Santarelli, B. Valtancoli, *Coord. Chem. Rev.* **2008**, *252*, 1052.

58 K. F. Bowes, I. P. Clark, J. M. Cole, M. Gourlay, A. M. E. Griffin, M. F. Mahon, L. Ooi, A. W. Parker, P. R. Raithby, H. A. Sparkes, M. Towrie, *CrstEngComm* **2005**, *7*, 269.

59 G. Pan, F. Chen, L. Hu, K. Zhang, J. Dai, F. Zhang, *Adv. Funct. Mater.* **2015**, *25*, 5126.

60 M. M. González, H. Osiry, M. Martínez, J. Rodríguez-Hernández, A. A. Lemus-Santana, E. Reguera, *J. Magn. Magn. Mater.* **2019**, *471*, 70.

61 D. A. Turchetti, P. C. Rodrigues, L. S. Berlim, C. Zanlorenzi, G. C. Faria, T. D. Z. Atvars, W. H. Schreiner, L. C. Akcelrud, *Synth. Met.* **2012**, *162*, 35.

62 M. González, A. A. Lemus-Santana, J. Rodríguez-Hernández, M. Knobel, E. Reguera, *J. Solid State Chem.* **2013**, *197*, 317.